

DESIGN AND EXPERIMENT OF SEGMENTABLE ADJUSTABLE THRESHING DEVICE FOR RICE SEED BREEDING

制繁种水稻分段可调脱粒装置设计与试验

Ranbing YANG^{1,2}, Qi LIU¹, Yiren QING^{*2}, Zhiguo PAN¹, Guoying LI³,
Shuai WANG¹, Peiyu WANG², Yalong SHU¹

¹ College of Electrical and Mechanical Engineering, Qingdao Agricultural University, Qingdao / China

² College of Mechanical and Electrical Engineering, Hainan University, Haikou / China

³ Qingdao Pulantech Machinery Technology Co., Ltd., Qingdao / China

Tel: +8618851400010; E-mail: Jsuyirenq@163.com

Corresponding author: Yiren Qing

DOI: <https://doi.org/10.35633/inmateh-75-23>

Keywords: Seed breeding, Concave screen, Threshing clearance, Low loss

ABSTRACT

In response to the current challenges in the harvesting process of hybrid rice, where the threshing gap cannot adequately adapt to the varying threshing requirements, leading to high grain breakage rates, loss rates, and frequent clogging of the drum, a new threshing device for hybrid rice was designed by adjusting the gap of the concave screen. The concave screen was divided into a low-loss threshing section and a low-damage threshing section, with the addition of a hydraulic system to enable the adjustment of the threshing gap. A dynamic analysis of the rice at the spiral feeding inlet and within the threshing drum was conducted, determining that the adjustable range of the threshing gap is between 10 and 20 mm. A prototype of the low-loss threshing device for hybrid rice was built, and bench tests were performed with feed rate, drum speed, and threshing gap as influencing factors, while cleaning rate and breakage rate were used as response indicators in an orthogonal experiment to determine the optimal parameter combination. The optimal threshing performance was achieved at a threshing gap of 14.19 mm, a drum speed of 460.12 r/min, and a feed rate of 2.13 kg/s, resulting in a cleaning rate of 97.67% and a breakage rate of 0.295%. Subsequent verification tests under the optimal combination showed a cleaning rate of 96.2% and a breakage rate of 0.36%, meeting the harvesting standards for hybrid rice. This research provides theoretical support for the development of mechanized harvesting equipment for hybrid rice.

摘要

针对目前制繁种水稻收获过程中脱粒间隙无法很好的适应不同条件下水稻脱粒需求，脱粒过程中水稻籽粒破碎率、损失率及滚筒易堵塞等问题，从调节凹板筛脱粒间隙的角度出发，设计了一种制繁种水稻脱粒装置。将凹板筛设计为低损失脱粒段与低损伤脱粒段，通过加入液压系统能够实现脱粒间隙调节。对水稻在螺旋喂入口和脱粒滚筒内进行动力学分析，确定了脱粒间隙可调范围为10~20mm。试制了制繁种水稻低损失脱粒装置试验台，进行台架试验，以喂入量、滚筒转速、脱粒间隙作为影响因素，以脱净率和破损率作为响应指标进行正交实验，确定最优组合参数，获得脱粒装置在脱粒间隙14.19mm、滚筒转速460.12r/min、喂入量2.13kg/s的组合参数下脱粒效果最优，脱净率为97.67%，破损率为0.295%，并在最优组合下验证试验，结果表明脱净率为96.2%，破损率为0.36%，满足水稻制繁种收获标准，该研究可为制繁种水稻机械化收获装备的研制提供理论支持。

INTRODUCTION

Rice, as one of China's important food and economic crops, had a planting area of 28,949 thousand hectares and a yield of 206.6 million tons in 2023, according to statistics from the National Bureau of Statistics (Wei Li et al., 2024; Tian L. et al., 2020; Guo L. et al., 2024). The widespread adoption of rice harvesting machines has saved labor and resources, improved the efficiency of rice harvesting, and played an important role in grain harvesting. In seed breeding, an important aspect of agricultural production, the requirements for seed vitality and grain threshing are more stringent compared to regular rice harvesting during the rice harvesting process. Currently, common field rice-wheat combine harvesters are widely used for rice seed breeding harvesting, which often leads to high threshing losses and severe seed breakage.

Threshing, as an indispensable process, may result in increased loss and breakage rates when working parameters are poorly configured due to changes in feed rate, making it difficult to meet threshing requirements under different conditions (Teng, Y. et al., 2020). Therefore, reducing grain loss and breakage rates during rice seed breeding harvesting has become an urgent issue.

In recent years, researchers both domestically and abroad have conducted numerous studies aimed at reducing grain loss and breakage rates. Vlăduț N.V. et al., (2022), presented a mathematical model to characterize the threshing and separation process in an axial-flow thresher. Their paper aimed to provide a theoretical foundation for optimizing thresher design and performance. Bergkamp et al., (2015), designed a constant-pressure concave screen that, by incorporating a hydraulic cylinder to adjust the piston rod extension, achieved the effect of manually adjusting the threshing clearance, preventing situations where grain loss occurs due to excessive feed rates, and concluded that the constant-pressure concave screen is superior to traditional concave screens. Vlăduț N.V. et al., (2023), found that the loss (p_{ev}) is affected by the threshing rotor speed (n), implicit rotor peripheral speed (v_p), material feed speed (v_a), the space between the rotor and the counter - rotor (δ), material feed flow (Q), material density (ρ), and the length of the threshing device (L). Since ρ and L remain constant, they analyzed the variation of the loss with respect to v_p , Q , ρ , and v_a . By changing two parameters of the loss function (presented graphically), the study aimed to minimize the loss. Ivan Gh. et al., (2015), demonstrated that by optimizing the feeding process, the capacity of the tangential threshing system can be enhanced. This is achieved when the system can guide more materials carried by the feeder house conveyor during a full rotation of the threshing cylinder. The research indicates that to improve the feeding capacity of the threshing system in conventional cereal harvesters, it is necessary to match the speed, quantity, and spacing of the feeder house conveyor slats with the number of rods on the threshing cylinder and the speed of the tangential threshing cylinder. Matousek et al., (2017), designed a three-section combined adjustable concave screen, composed of three small concave screens as a whole, with the movement of the three small concave screens controlled by rotating connecting shafts, concluding that adjusting the threshing clearance can reduce loss rates. Miu, P.I. & Kutzbach et al, (2007) analyzed the movement trajectory of rice in the threshing device, established a kinematic mathematical model based on crop position and movement speed, determined the movement laws of rice in the threshing device, providing a theoretical basis for analyzing the proportion of grains and extraneous matter in the threshing device. Osueke et al, (2011), analyzed the effects of grain threshing force, threshing clearance, feed rate, and drum speed on the threshing process, optimizing the threshing analysis model and concluding that the threshing clearance and grain threshing force are the main factors affecting threshing quality. Dai, F. et al, (2011), designed a vertical axis flow cone-type threshing device by adding a conical short bar-tooth plate structure on the drum, concluding that this method accelerates the axial transport speed of breeding wheat and is less prone to blockages. Lian Y. et al, (2020), designed an adaptive control system for the threshing system of a rice-wheat combine harvester, concluding that the operational parameter control system effectively improves harvesting efficiency by studying the adaptive control system and comparing harvesting tests with and without controllers. Zhang Lu Ke et al, (2022), proposed a rice threshing and separating device blockage monitoring and diagnostic system, effectively preventing grain loss caused by drum blockages. Liu Wanru et al, (2023), established an impact mechanics model for collisions between rice grains and different threshing elements, concluding that the optimized curved rod tooth drum effectively reduces the power consumption of the drum and enhances the threshing performance. Teng Yuejiang et al, (2020), designed a segmented vertical flow threshing and separating device, providing a reference for the improvement and optimization of the threshing device of vertical flow rice harvesters through multi-objective optimization experiments aimed at problems such as high breakage rates, incomplete threshing, and inadequate separation.

In conclusion, current research on rice threshing devices primarily focuses on adjusting the overall threshing clearance of the device through the drum and concave screen. However, the inability to simultaneously meet the threshing conditions at the front and rear ends of the threshing device due to differences in grain density inside the device caused by feed rates hinders the reduction of grain loss and breakage rates. Therefore, in response to issues such as grain loss and breakage during rice seed breeding harvesting, this paper proposes the design of a threshing device for rice seed breeding, analyzes the movement patterns of rice during threshing, and, based on single-factor and multi-factor experiments, identifies the optimal operating parameters, aiming to provide a reference for the development of harvesting equipment for rice seed breeding trials.

MATERIALS AND METHODS

Overall Structure

The overall structure of the harvesting and threshing device for hybrid rice is shown in Figure 1. It mainly consists of a material transport device, material feeding port, cover plate, concave screen, threshing drum, backing plate, hydraulic cylinder, motor, and power transmission device, among others. The main parameters of the device are presented in Table 1.

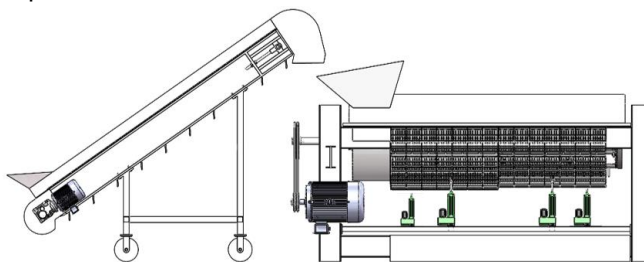


Fig. 1 – The overall structure of the segmented adjustable threshing device for hybrid rice harvesting

Table 1

The main parameters of the segmented adjustable threshing device for rice harvesting	
Parameter	Numerical value
Test bench dimensions (Length × Width × Height) / (m × m × m)	2.2×1.1×1.5
Length of concave screen (m)	1.8
Engine power (kW)	103
Type of concave screen	Grid type
Threshing gap adjustment range (mm)	5~10

When the threshing device begins to operate, rice is transported through the material conveying device into the spiral feeding inlet. From the spiral feeding inlet, it enters the threshing device for threshing, using a radial feeding and discharging method. The motor provides power to drive the power transmission device, which in turn drives the threshing drum to rotate and supports the concave screen's extension and retraction with the hydraulic cylinder. Under the combined action of the threshing drum and the concave screen, the rice undergoes multiple forces such as gravity, impact force, friction force, and centrifugal force to achieve the separation of grains from the stalks. Sensors within the threshing device are used to detect the feeding amount and grain density inside the drum, controlling the extension and retraction of the hydraulic cylinder to drive the two parts of the concave screen to move independently, adjusting the threshing gap. Ultimately, the rice grains fall into the grain bin, while impurities are discharged outside the threshing device, completing the threshing process.

Design and selection of key components

The threshing device of traditional rice harvesting machines has a fixed concave screen that is not adjustable, which cannot better meet the threshing requirements under different working conditions. When the feeding amount is too large, the grain density inside the threshing device increases, causing the rice material in the threshing drum to spiral forward in the feeding direction. As a result, the grain density in the front half of the threshing device is greater than that in the rear half, leading to a situation where an excessively large threshing gap reduces the cleaning rate, while an excessively small threshing gap increases the damage rate. To address this issue, a hydraulic system is introduced to support the concave screen and divide it into a low-loss threshing segment and a low-damage threshing segment, allowing for independent control of the two sections. This enables the adjustment of the appropriate threshing gap based on the varying grain densities, thus solving the problems of reduced cleaning rates and increased damage rates caused by uneven grain density within the threshing drum.

Dynamic analysis of rice at the helical feeding inlet

The spiral feed inlet serves as the starting point for rice entering the threshing device (Xu L., Li Y., & Ding L. et al, 2008), enabling the stable transport of rice into the threshing drum. To prevent blockages in the drum and grain loss caused by excessive feeding, a dynamic analysis of the rice is conducted at any point along the spiral feed inlet. As shown in Figure 2, the rice plant is treated as a particle O for the dynamic analysis within the spiral feed inlet. To ensure that the material moves along the spiral feed inlet and smoothly enters the threshing drum, the following conditions must be met:

$$T \cos \alpha > F_b \sin \alpha \tag{1}$$

$$F_b = f_1 T = T \tan \beta \tag{2}$$

In the formula, f_1 is the coefficient of friction between the material and the spiral feed inlet.

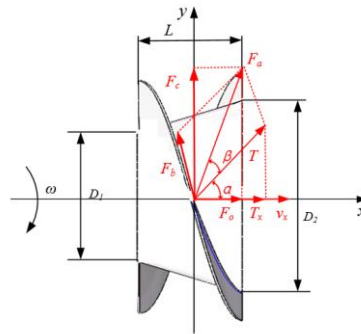


Fig. 2 – Kinetic analysis of rice at the screw feed inlet

where: ω is the angular velocity of rotation of the threshing drum, rad/s; D_1 is the diameter of the front end of the screw feeding inlet, cm; L is the length of the screw feeding inlet, cm; D_2 is the diameter of the rear end of the screw feeding inlet, cm; F_b is the friction between the rice and the screw feed inlet, N; T is the conveying force of the screw feed inlet to the rice, N; T_x is the component of T on the x-axis, N; F_a is the resultant force of F_b and T , N; F_o is the component of F_a on the x-axis, N; F_c is the component of F_a on the y-axis, N; v_x is the axial feeding speed of rice, m/s; α is the friction angle between the rice and the screw feed inlet, °; β is the helix angle of the screw feed inlet, °.

From equations (6) and (7), it can be concluded that to ensure the material moves axially along the spiral feed inlet, the axial thrust force must exceed the axial resistance, that is:

$$\cot \alpha > \tan \beta \tag{3}$$

Therefore, the β between the helix angle and the friction angle α should meet:

$$\alpha < \frac{\pi}{2} - \beta \tag{4}$$

As the main influencing factor of rice feeding speed v_x (Zeng, S., Zeng, L. et al, 2022), the helix angle β decreases when the β increases, the axial component T_x of T decreases, the feeding power P increases, the feeding speed decreases, and the feeding efficiency decreases. When β decreases, the axial component T_x of T increases, the feeding speed increases, and the feeding efficiency increases. In order to select the appropriate helix angle β , prevent the drum from clogging, and improve the feeding efficiency, the following are required:

$$P = T_x v_x \tag{5}$$

$$v_x = \omega r \tag{6}$$

In the formula, ω is the angular velocity of the drum, in rad/s; r is the radius of the drum, in mm.

Upon measurement, the friction α is 48.3°. According to equations (4), (5), and (6), the helical angle β is set to 35°.

Parameter design of the threshing drum

The structure of the threshing drum is shown in Figure 3. The threshing of rice is mainly accomplished through the cooperation between the rods and teeth of the threshing drum and the concave sieve. Considering that the moisture content of southern rice is relatively high, which can easily lead to damage during threshing, this paper selects cylindrical threshing rods to reduce the contact area with the rice, thereby lowering the damage rate. The length of the rods is 78 mm, and the distance between adjacent rods is 82 mm.

The diameter of the threshing drum determines the threshing trajectory. A smaller drum diameter reduces the threshing line speed, decreases the threshing capacity, and lowers the clean threshing rate of the rice. Conversely, a larger drum diameter increases the threshing line speed, enhances the threshing capacity, and raises the damage rate of the rice. Based on domestic standards for cylindrical threshing drums, the diameter D of the threshing drum is determined to be 500 mm.

The length L_l of the threshing drum is designed as:

$$L_l = \frac{q}{q_1} \tag{7}$$

In the formula, q is the feed rate, in kg/s, and q_1 is the threshing capacity of the drum per unit volume, in kg/(s·m).

The threshing device uses cylindrical rods, with q_1 set at 1 to 1.5 kg/(s·m) and q set at 2.5 kg/s. The length of the threshing drum is determined to be 2200 mm using formula (7).

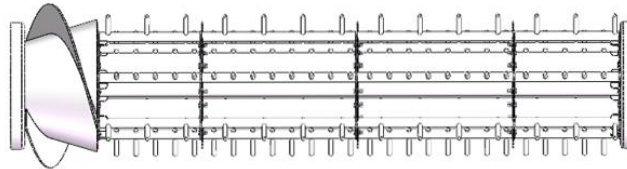


Fig. 4 – Structure diagram of threshing drum

Kinematic analysis of rice in the threshing drum

Due to the complex forces acting on rice during the threshing process, a dynamic analysis of rice threshing is conducted at low speeds to select an appropriate range for the threshing gap and drum rotational speed, thereby reducing damage to the rice grains. A coordinate system (xoy) is established with the center of gravity of the rice as the origin to analyze the force distribution on the rice, as shown in Figure 4.

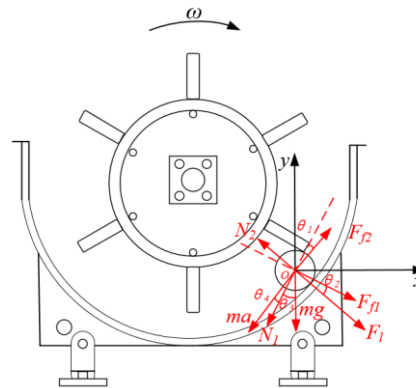


Fig. 5 – Kinetic analysis of rice in threshing drum

where: ω is the angular velocity of the threshing drum, in rad/s; N_1 is the impact force of the threshing rod teeth on the rice, in N; N_2 is the supporting force of the concave sieve on the rice, in N; F_{f1} is the frictional force between the threshing rod teeth and the rice, in N; F_{f2} is the frictional force between the concave sieve and the rice, in N; F_i is the centrifugal force acting on the rice, in N; m is the mass of the rice, in g; g is the gravitational acceleration, in N/kg⁻¹; a is the acceleration of the rice, in m/s²; θ_1 is the angle between the impact force N_1 and the frictional force F_{f2} , in degrees; θ_2 is the angle between the frictional force F_{f1} and the centrifugal force F_i , in degrees; θ_3 is the angle between the gravitational force mg and the impact force N_1 , in degrees; θ_4 is the angle between the direction of the rice’s acceleration and the impact force N_1 , in degrees.

According to Figure 5, the force analysis of rice during the threshing process is shown in formulas (8) and (9).

$$N_1 + ma \cos \theta_4 + mg \cos \theta_3 + F_i \sin \theta_2 = F_{f2} \cos \theta_1 + N_2 \sin \theta_2 \tag{8}$$

$$F_{f1} + F_i \cos \theta_2 + mg \sin \theta_3 + F_{f2} \sin \theta_1 = N_2 \cos \theta_2 + ma \sin \theta_4 \tag{9}$$

$$F_i = mr\omega^2 \tag{10}$$

$$F_{f1} = \mu_1 N_1 \tag{11}$$

$$F_{f2} = \mu_2 N_2 \tag{12}$$

In the formulas, r represents the rotation radius of the rice, in mm. μ_1 and μ_2 are the coefficients of friction between the rice and the threshing rod teeth and concave sieve, respectively, with $\mu_1 = 0.59$ and $\mu_2 = 0.54$.

Kinematic analysis of rice in the threshing drum

Before threshing the grains, the threshing device must first separate the rice from the straw. The grains are rubbed and peeled by passing through the threshing drum and concave sieve, then they enter the cleaning device through the concave sieve. Under the influence of the threshing drum and the flow guide plate, the straw moves forward in a spiral manner and is eventually discharged from the end of the threshing device (Chen L. et al, 2023; Chen J. et al., 2024; Wang J. et al., 2021).

To explore the motion laws of the material within the threshing device and ensure that the material moves axially within the threshing drum, preventing blockages and allowing for smooth discharge, an xoy coordinate system is established with the center of mass of the straw as the origin, as shown in Figure 6.

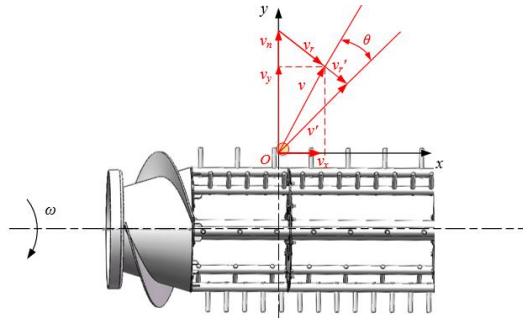


Fig. 6 – Kinematics analysis of straw in threshing device

where:

ω is the angular velocity of the threshing drum, in rad/s; v is the actual motion speed of the straw, in m/s; v_x is the component of speed v along the x-axis, in m/s; v_y is the component of speed v along the y-axis, in m/s; v_n is the pulling speed under the influence of the flow guide plate, in m/s; v_r is the sliding speed of the straw relative to the flow guide plate, in m/s; v_r' is the sliding speed in the absence of friction, in m/s; v' is the motion speed in the absence of friction, in m/s; θ is the angle of change in speed due to the action of friction, in degrees.

As shown in Figure 6, the velocity decomposition of the rice straw within the threshing device is represented by equations (15) and (16).

$$v_x = \frac{dn \left(\mu_3 + \frac{d}{2\pi r} \right)}{60 \left[1 + \left(\frac{d}{2\pi r} \right)^2 \right]} \quad (15)$$

$$v_y = \frac{dn \left(1 - \frac{\mu_3 d}{2\pi r} \right)}{60 \left[1 + \left(\frac{d}{2\pi r} \right)^2 \right]} \quad (16)$$

where: d is the pitch of the guide plate, in mm; n is the rotational speed of the drum, in rad/s; μ_3 is the coefficient of friction between the straw and the guide plate, where $\mu_3 = 0.18$; r is the radius of the drum, in mm.

From equations (15) and (16), it can be seen that the motion speed of the straw is related to the pitch of the guide plate, the rotational speed of the drum, and the radius of the drum. When the central axis of the drum is fixed and the radius of the drum increases while the length of the threshing rod teeth remains unchanged, it can be approximated that the threshing gap increases. In this paper, the change in the radius of the drum is used to represent the change in the threshing gap.

When the drum rotational speed n increases, v_x and v_y also increase. This can be interpreted as an enhanced ability to separate grains from straw with the increasing drum speed, resulting in an increase in the instantaneous speed of the straw and a faster axial movement. When the radius of the drum r increases, the threshing gap enlarges, causing v_x and v_y to decrease, which can be explained as a reduction in the ability to separate rice grains from straw due to the enlargement of the threshing gap. When the pitch of the guide plate d increases, v_x and v_y decrease, which can be interpreted as a reduced conveying capacity for the straw with the increase in pitch, making it easier for the drum to become clogged.

In summary, to prevent the drum from clogging and to ensure the smooth progress of the threshing process, the drum rotational speed should be set between 260 and 660 r/min, and the threshing gap should be set between 10 and 20 mm.

Design of the concave plate sieve

During the threshing process, the concave plate sieve works in cooperation with the threshing drum to achieve the preliminary separation of rice grains and broken materials (Teng Y. *et al*, 2020). Traditional rice harvesters often have fixed structures for the concave plate sieve, and the fixed threshing gap cannot adapt to different working conditions, which can easily cause damage to the rice grains. Therefore, a segmented adjustable concave plate sieve has been designed, as shown in Figure 7. Based on the existing dimensions of the threshing segment of the threshing drum, this paper selects a bar-type concave plate sieve to increase grain passage, reduce collision intensity, and lower the damage rate. The length of the concave plate sieve is set at 2100 mm, divided into two parts, each measuring 1050 mm (Di Q. *et al*, 2021). The bars are made of steel plates that are 1010 mm long and 22 mm wide, with a wrap angle of 190°.

Two pads are installed in each part to connect the hydraulic cylinder with the concave plate sieve. When there are many grains, increasing the gap of the concave plate can effectively reduce the collision intensity between the concave plate sieve and the rice grains, while providing enough space for high-density rice to be threshed. Increasing the threshing gap not only improves the passage of grains but also reduces the damage caused by the squeezing of grains due to the clogging of the threshing device.

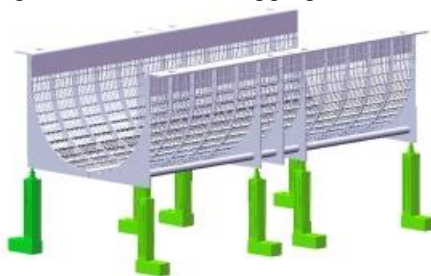


Fig. 7 – Structure diagram of concave plate screen

The hydraulic system, serving as the power device for adjusting the threshing gap, is designed with two oil inlets and sixteen oil outlets, ensuring simultaneous supply to four hydraulic cylinders with an error margin of less than 2%. When there is a need to adjust the threshing gap, the hydraulic system directs hydraulic oil into the hollow hydraulic cylinders through hydraulic rotary joints, with one side featuring a piston rod. By controlling the flow of hydraulic oil, the piston rod extends and retracts, thereby driving the movement of the concave plate sieve to modify the size of the threshing gap. When adjustment of the threshing gap is unnecessary, the hydraulic oil flow ceases, maintaining the piston rod of the hydraulic cylinder in a stationary state. The hydraulic system also remains static, ensuring that the position of the concave plate sieve does not change, thus guaranteeing a constant threshing gap.

The design of the adjustable hydraulic system allows for precise control when there is a need to modify the threshing gap, while maintaining stability when no adjustments are required.

Bench test and result analysis

To verify the working effect of the segmented adjustable threshing device, a test stand was fabricated for conducting bench tests. The test subjects selected were Shuyou No. 9 rice from the rice planting base in Xinlong Town, Dongfang City, Hainan Province, with basic parameters shown in Table 2.

Table 2

Parameters of basic physical characteristics of rice	
Parameter	Numerical value
Moisture content of rice grains / %	23.1
Moisture content of rice straw / %	74.4
Height of rice plant / cm	103.6
Thousand grain weight / g	27.1
Number of grains per ear	154

Experimental method

This experiment combines the design analysis of key component parameters, selecting threshing gap A, drum speed B, and feeding amount C as experimental factors, and selecting cleaning rate y_w and damage

rate y_p as evaluation indicators. Based on GB/T 5982-2017 "Test Methods for Threshers" and DB37/T2878.2-2016 "General Technical Requirements for Agricultural Product Harvesting Machinery", an orthogonal experiment is conducted.

The calculation formulas for cleaning rate y_w and damage rate y_p are as follows:

$$y_w = \frac{m_w}{m} \times 100\% \tag{17}$$

In the formula,

y_w is the cleaning rate, %; m_w is the weight of threshed grains, g; m is the total grain mass, g.

$$y_p = \frac{m_p}{m} \times 100\% \tag{18}$$

In the formula,

y_p is the damage rate, %; m_p is the weight of damaged grains, g; m is the total grain mass, g.



Fig. 8 – Test bench of segmented adjustable threshing device for rice harvesting

Single-factor experiment

Before conducting the orthogonal experiment, single-factor experiments should be carried out on the threshing gap A, drum speed B, and feeding amount C to determine the reasonable range of factor levels and the influence patterns of each factor on the threshing performance. Based on preliminary trials and the adjustable range of the device, the single-factor experimental ranges are set as follows: threshing gap A is 10–20 mm, drum speed B is 260–660 r/min, and feeding amount C is 1–3 kg/s.

When the threshing gap A is fixed at 15 mm, the drum speed B is set at 450 r/min, and the feeding amount ranges from 1 to 3 kg/s, the effects of feeding amount C on the cleaning rate y_w and damage rate y_p during the threshing process are shown in Figure 9. As illustrated in Figure 9, when the feeding amount is between 1–2 kg/s, both the cleaning rate and damage rate increase significantly with the rise in feeding amount; the cleaning rate rises from 93.1% to 99.2%, while the damage rate increases from 0.18% to 0.59%. However, when the feeding amount is between 2–3 kg/s, the cleaning rate shows a downward trend, decreasing from 99.25% to 94.5%. An excessively high feeding amount results in the threshing device being unable to effectively thresh the rice, leading to a decline in threshing efficiency, while the damage rate slowly increases from 0.59% to 0.8%. To ensure effective threshing, the selected feeding amount range is 1.5–2.5 kg/s.

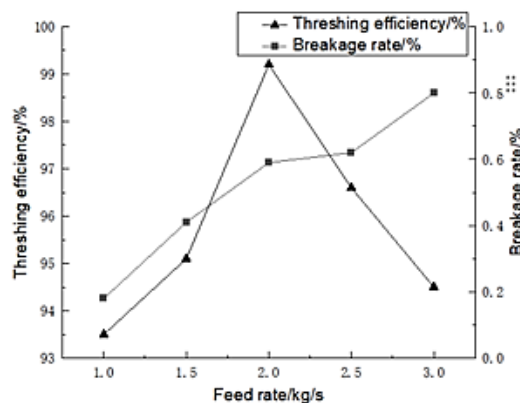


Fig. 9 – The impact of feed rate on threshing efficiency and damage rate

When the threshing gap A is fixed at 15 mm, the drum speed B ranges from 260 to 660 r/min, and the feeding amount is 2 kg/s, the effects of drum speed B on the cleaning rate y_w and damage rate y_p during the threshing process are shown in Figure 10. As illustrated in Figure 10, with the continuous increase in the drum speed, both the cleaning rate and loss rate show an overall upward trend. When the drum speed increases from 450 r/min to 550 r/min, the cleaning rate rises from 94.2% to 99.4%, indicating a significant upward trend. During this process, as the drum speed increases, the impact force on the rice becomes more pronounced, resulting in effective threshing. However, when the drum speed increases from 550 r/min to 660 r/min, the cleaning rate drops from 99.4% to 98.7%. The excessively high drum speed fails to achieve optimal threshing results, leading to grain loss. To ensure effective threshing, the selected drum speed range is set at 450–550 r/min.

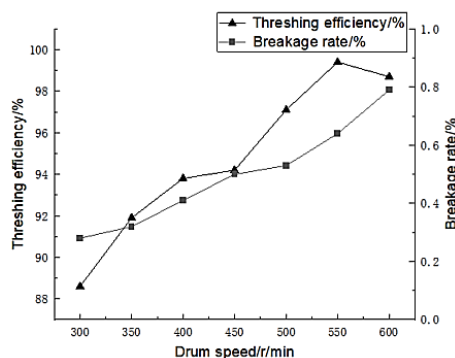


Fig. 10 – The impact of roller speed on cleaning rate and damage rate

When the threshing gap A is set between 10–20 mm, the drum speed B ranges from 260 to 660 r/min, and the feeding amount is 2 kg/s, the effects of threshing gap A on the cleaning rate y_w and damage rate y_p during the threshing process are illustrated in Figure 11. As shown in Figure 11, when the threshing gap is between 10–15 mm, the cleaning rate exhibits an upward trend, increasing from 95.5% to 99.6%. A good threshing gap allows the threshing rod teeth to fully contact the rice and effectively rub off the husk, thereby improving the threshing effect. At the same time, it reduces the collisions between the rice grains and the concave screen, with the damage rate decreasing from 0.95% to 0.32%. However, when the threshing gap is between 15 mm and 20 mm, the cleaning rate shows a downward trend, dropping from 99.6% to 94.3%. A larger threshing gap is unable to efficiently complete the threshing of rice, resulting in some rice not being fully rubbed and husked, which causes losses. Additionally, this leads to insufficient contact and collisions between the rice grains and the concave screen, causing the damage rate to further drop from 0.32% to 0.08%. To ensure effective threshing, the selected threshing gap range is set at 12–18 mm.

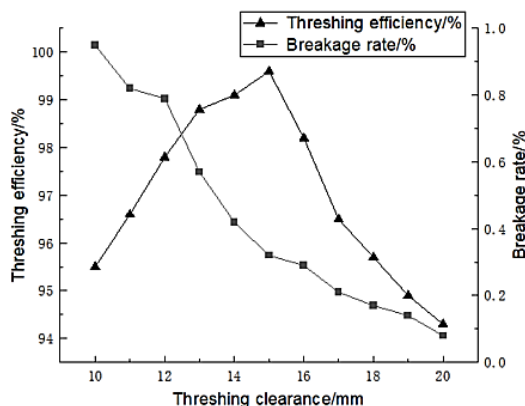


Fig. 11 – The impact of threshing gap on threshing purity and damage rate

RESULTS AND ANALYSIS

The experiment utilized a quadratic orthogonal design (Yang, R. et al., 2024), with the experimental factors being threshing gap A, drum speed B, and feeding amount C. The experimental indicators were the cleaning rate y_w and damage rate y_p . Based on the analysis of the previous experimental results, the value ranges for each experimental factor were determined: the threshing gap A is set at 12–18 mm, the drum speed B at 450–550 r/min, and the feeding amount C at 1.5–2.5 kg/s. The coding table for the levels of the experimental factors is shown in Table 3, and the experimental plan and results are presented in Table 4.

Table 3

Factor level coding table				
Material	Threshing gap A	Drum speed B	Feeding amount C	
-1	12	450	1.5	
0	15	500	2	
1	18	550	2.5	

Table 4

Test protocol and results						
Experiment number	Threshing gap	Drum speed	Feeding amount	Cleaning rate	Damage rate	
	A	B	C	/ %	/ %	
1	12	550	2	94.89	0.45	
2	15	450	1.5	99.51	0.22	
3	18	500	1.5	97.69	0.15	
4	15	500	2	98.25	0.33	
5	15	500	2	98	0.3	
6	15	550	2.5	97.18	0.37	
7	12	450	2	95.05	0.33	
8	18	450	2	97.99	0.17	
9	18	500	2.5	96.61	0.15	
10	15	500	2	98.98	0.31	
11	12	500	2.5	95.24	0.41	
12	15	500	2	98.69	0.29	
13	15	450	2.5	96.69	0.24	
14	15	550	1.5	95.9	0.3	
15	15	500	2	98.1	0.28	
16	18	550	2	96.48	0.17	
17	12	500	1.5	95.74	0.32	

Using Design-Expert software, a quadratic regression analysis and multiple regression fitting were performed on the experimental data (Tian L. et al., 2020), along with variance analysis and significance testing of the experimental factors. As shown in Table 5, the experimental results indicate that the overall model for cleaning rate y_w and damage rate y_p is significant ($P < 0.01$), and the regression equation model for cleaning rate y_w and damage rate y_p is highly significant. Factors A, B, BC, and A^2 have a highly significant effect on cleaning rate y_w ($P < 0.01$), while factors C and B^2 have a significant effect on cleaning rate y_w ($0.01 \leq P < 0.05$). Factors AB, AC, and C^2 have no significant effect on cleaning rate y_w ($P \geq 0.05$). Similarly, factors A, B, BC, and A^2 have a highly significant effect on damage rate y_p ($P < 0.01$), while factors C and B^2 have a significant effect on damage rate y_p ($0.01 \leq P < 0.05$). Factors AB, AC, and C^2 have no significant effect on damage rate y_p ($P \geq 0.05$). The insignificant factors were included in the residual term, resulting in the regression equations for cleaning rate y_w and damage rate y_p as follows:

$$y_w = 8.99 + 7.15A + 0.2B - 12.89C + 0.041BC - 0.18A^2 - 0.26 \times 10^{-3} B^2 \tag{19}$$

$$y_p = -1.88 + 0.17A + 0.22 \times 10^{-2} B + 0.36C - 0.2 \times 10^{-3} AB - 0.015AC - 0.26 \times 10^{-2} \tag{20}$$

As shown in Table 5, the cleaning rate y_w and damage rate y_p have $P < 0.01$, indicating that the regression model is highly significant; the lack of fit term $P_w = 0.5313$ and $P_p = 0.5063$ ($P > 0.1$) are not significant. The regression equation fits well for both the cleaning rate and damage rate, with no other major factors affecting the experimental indicators. The quadratic relationship is significant, and the analysis results are reasonable.

Table 5

Analysis of variance (ANOVA) of decontamination rate and breakage rate										
Source	Cleaning Rate					Damage Rate				
	Sum of Squares	Deg. of Freedom	Mean Square	F Value	P Value	Sum of Squares	Deg. of Freedom	Mean Square	F Value	P Value
Model	31.63	9	3.51	21.60	0.0003	0.1229	9	0.0137	38.17	<0.00001
A	7.70	1	7.70	47.34	0.0002	0.0946	1	0.0946	264.39	<0.00001
B	2.87	1	2.87	17.63	0.0040	0.0136	1	0.0136	38.04	0.0005
C	1.22	1	1.22	7.48	0.0291	0.0040	1	0.0040	11.32	0.0120
AB	0.46	1	0.46	2.80	0.1382	0.0036	1	0.0036	10.06	0.0157
AC	0.084	1	0.084	0.52	0.4955	0.0020	1	0.0020	5.66	0.0490

Source	Cleaning Rate					Damage Rate				
	Sum of Squares	Deg. of Freedom	Mean Square	F Value	P Value	Sum of Squares	Deg. of Freedom	Mean Square	F Value	P Value
BC	4.20	1	4.20	25.83	0.0014	0.0006	1	0.0006	1.75	0.2279
A ²	11.47	1	11.47	70.52	0.0001	0.0023	1	0.0023	6.50	0.0382
B ²	1.78	1	1.78	10.96	0.0129	0.0415	1	0.0415	0.03	0.8753
C ²	0.79	1	0.79	4.86	0.0634	0.0019	1	0.0019	5.19	0.0568
Residual	1.14	7	0.1627			0.0025	7	0.0019		
Deviance	0.45	3	0.1487	0.8583	0.5313	0.0010	3	0.0003	0.9234	0.5063
Total Sum	32.77	16				0.1254	16			

Response surface methodology

To observe the effects of threshing gap, drum speed, and feeding rate on the cleaning rate and damage rate of hybrid rice grain harvested, this study fixes the level of one factor and investigates the interaction between the other two factors.

Through interaction response surface analysis (Ge Y. et al., 2015), the first figure in Figure 12 shows the response cloud of the cleaning rate (y_w) under the interaction of drum speed and feeding rate. It can be seen from the figure that when the threshing gap is 15 mm, as the drum speed and feeding rate increase, the cleaning rate begins to rise. This phenomenon can be attributed to the fact that the increase in drum speed enhances the force exerted by the threshing elements on the rice, allowing for successful threshing and consequently leading to an increase in the cleaning rate. From this interaction response cloud, it can be concluded that the effect of drum speed on the cleaning rate is significantly greater than that of feeding rate on the cleaning rate.

Similarly, through interaction response surface analysis, the second figure in Figure 12 shows the response cloud of the damage rate (y_p) under the interaction of threshing gap and drum speed. It can be observed that when the feeding rate is 2 kg/s, as the threshing gap and drum speed increase, the damage rate decreases. This phenomenon can be explained by the fact that the increase in threshing gap enlarges the internal space of the threshing device, reducing the force at the contact point between the grains and the concave screen under the action of the threshing drum, thereby leading to a decrease in the damage rate of the grains. However, with the increase in drum speed, the damage rate increases due to the greater force exerted on the rice when it contacts the threshing elements, which may cause damage to the grains if the drum speed is too high during threshing. The interaction response cloud indicates that the effect of threshing gap on the damage rate is clearly greater than that of drum speed on the damage rate.

Through interaction response analysis, the third figure in Figure 12 shows the response cloud of the damage rate (y_p) under the interaction of threshing gap and feeding rate.

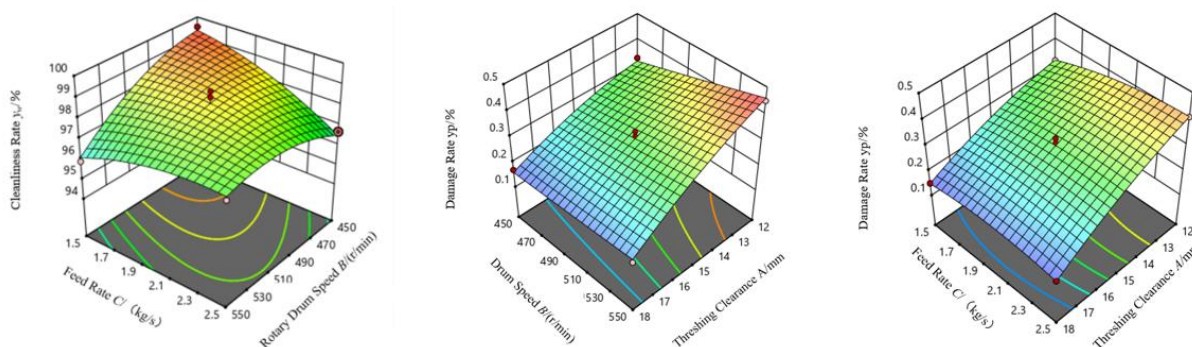


Fig. 12 – Interaction Response Plot

It can be seen that when the drum speed is 500 r/min, as the threshing gap and feeding rate increase, the damage rate decreases. This phenomenon can be explained by the fact that the increase in threshing gap enlarges the internal space of the threshing device, reducing the force at the contact point between the grains and the concave screen under the action of the threshing drum, thus leading to a decrease in the damage rate of the grains. As the feeding rate increases, the damage rate rises slightly, but the change is not significant, which can be attributed to the increased material density within the threshing device and the greater interaction

force between materials, resulting in slight damage. Therefore, it is evident that the impact of the threshing gap on the damage rate is significantly greater than that of the feeding rate on the damage rate.

Determination of optimal parameters

To increase the cleanliness rate (y_w) and reduce the damage rate (y_p), the maximization of cleanliness rate and minimization of damage rate are set as optimization objectives, seeking the best operating parameters, as shown in equation (19):

$$\begin{cases} \max y_w(A, B, C) \\ \min y_p(A, B, C) \\ 12 < A < 18 \\ 450 < B < 550 \\ 1.5 < C < 2.5 \end{cases} \quad (19)$$

Through optimization, the optimal parameters obtained are: threshing clearance of 14.19 mm, rotary drum speed of 460.11 r/min, and feed rate of 2.13 kg/s, resulting in a cleanliness rate of 97.67% and a damage rate of 0.295%, which meet the relevant threshing standards.

The adjusted parameters for the platform are: threshing clearance of 14.2 mm, rotary drum speed of 460 r/min, and feed rate of 2.1 kg/s. Experimental results indicate a cleanliness rate of 96.2% and a damage rate of 0.36%, with a relative error of less than 2 percentage points compared to the model optimization results.

CONCLUSIONS

(1) In response to the current challenges in the harvesting process of hybrid rice, where the threshing clearance cannot adequately adapt to the threshing requirements under different conditions, issues such as grain breakage rate, loss rate, and drum clogging during threshing are addressed. A threshing device for hybrid rice is designed from the perspective of adjusting the threshing clearance of the concave screen.

(2) A kinematic analysis of the threshing process is conducted. By analyzing the forces acting on the rice at the spiral feeding inlet and within the threshing drum, the selection of the concave screen and threshing drum is determined, aiming to reduce grain damage during threshing. Additionally, single-factor experiments are performed to establish the threshing clearance range of 12 to 18 mm, the drum speed range of 450 to 550 r/min, and the feed rate range of 1.5 to 2.5 kg/s.

(3) Using threshing clearance, drum speed, and feed rate as experimental factors, and cleanliness rate and damage rate as response indicators, an orthogonal experiment is conducted to establish a regression model for the relationship between threshing clearance, drum speed, feed rate, cleanliness rate, and damage rate. The results indicate that at a threshing clearance of 14.19 mm, a drum speed of 460.11 r/min, and a feed rate of 2.13 kg/s, the cleanliness rate is 97.67% and the damage rate is 0.295%. Verification through platform experiments shows that the cleanliness rate is 96.2% and the damage rate is 0.36%, with a relative error of less than 2% compared to the model optimization results. This demonstrates that this parameter combination can effectively improve the cleanliness rate of rice grains and significantly reduce the damage rate of rice grains.

ACKNOWLEDGEMENT

The authors were funded for this project by the National Key R&D Program of China, Research and Development of Low-loss and High-Purity Intelligent Harvesting Technology and Equipment for Rice Production and Multiplication (Project No. 2023YFD2000404-3) and Key R&D Project of Hainan Province (Project No. ZDYF2024XDNY181) and National Natural Science Foundation of China - Youth Science Foundation Project (Project No.52305252)

REFERENCES

- [1] Bergkamp, A., Regier. (2015). *Constant pressure concave assembly in a combine harvester processing system* (U.S. Patent No. 9220200B2).
- [2] Chen, J., Hao, S., Wang, C., Tang, Z., & Gu, X. (2024). Design of state monitoring and fault diagnosis system for combine harvester (联合收割机脱粒状态监测及故障诊断系统设计). *Journal of Agricultural Mechanization Research*, 46(07), 115–120.

- [3] Chen, L., Li, Y., Su, Z., Liu, Y., & Yin, Q. (2023). Design and test of a single-action variable-diameter threshing drum with rack (一种齿杆单动变直径脱粒滚筒的设计与试验). *Journal of Agricultural Mechanization Research*, 45(05), 43–48.
- [4] Dai, F., Gao, A., Sun, W., Zhang, F., Wei, H., & Han, Z. (2011). Design and experiment on longitudinal axial conical cylinder threshing unit (纵轴流锥型滚筒脱粒装置设计与试验). *Transactions of the Chinese Society for Agricultural Machinery*, 42(01), 74–78.
- [5] Di, Q. (2021). *Analysis and optimization design of threshing device for combine harvester (联合收割机脱粒装置分析及优化设计)* Xi'an University of Technology.
- [6] Ge, Y., Liang, Q., & Wang, G. (2015). *Experimental design method and Design-Expert software application (试验设计方法与 Design-Expert 软件应用)* Harbin: Harbin Institute of Technology Press.
- [7] Guo, L., Zhu, B., Han, Z., & Zhou, Q. (2024). Development status and suggestions of rice mechanized harvesting loss reduction technology (水稻机械化收获减损技术发展现状与建议). *Agricultural Equipment Technology*, 50(2), 4-6+9.
- [8] Ivan, Gh., Vlăduț, V., Ganea, I. (2015). Improving threshing system feeding of conventional cereal harvesting combine, *Proceedings of the 43 International Symposium on Agricultural Engineering "Actual Tasks on Agricultural Engineering"*, pp. 431-440, Opatija / Croatia.
- [9] Lian, Y. (2020). *Study on adaptive control system of operating parameters for threshing device of rice wheat combine harvester (稻麦联合收获机脱粒装置作业参数自适应控制系统研究)*. Jiangsu University.
- [10] Liu, W., Zhou, Y., Xu, H., Fu, J., Zhang, N., Xie, G., & Zhang, G. (2023). Optimization and experiments of the drum longitudinal axial threshing cylinder with rod tooth for rice (水稻鼓形纵轴流脱粒滚筒杆齿优化与试验). *Transactions of the Chinese Society of Agricultural Engineering*, 39(15), 34–45.
- [11] Matousek, R. A., & Claerhout, R. (2017). *Three section threshing concave configuration and adjustment mechanism for an agricultural harvesting combine* (U.S. Patent No. 20170164559A1).
- [12] Miu, P.I., & Kutzbach, H.D. (2007). Mathematical model of material kinematics in an axial threshing unit. *Computers and Electronics in Agriculture*, 58, 93–99.
- [13] Osueke, E. (2011). Simulation and optimization modeling of performance of a cereal thresher. *International Journal of Engineering & Technology*, 11(3), 143–152.
- [14] Teng, Y., Jin, C., Chen, Y., Liu, P., Yin, X., Wang, T. (2020). Design and optimization of segmented threshing device of combine harvester for rice and wheat (稻麦联合收获机分段式脱粒装置设计与优化). *Transactions of the Chinese Society of Agricultural Engineering*, 36(12), 1-12.
- [15] Tian, L., Li, H., & Hu, H. (2020). Design and experiment on coaxial double speed threshing for combine harvester (同轴双滚筒联合收获机设计与试验). *Transactions of the Chinese Society for Agricultural Machinery*, 51(S2), 139-146.
- [16] Tian, L., Zhang, Z., Lü, M., Jin, R., & Xiong, Y. (2020). Design and performance experiments of new threshing and separating device for head feeding combine harvester (半喂入联合收割机双速回转脱分装置设计与性能试验) *Journal of Chinese Agricultural Mechanization*, 41(09), 8-15.
- [17] Vlăduț, N.V., Biris, S.St., Cârdei, P., Găgeanu, I., Cujbescu, D., Ungureanu, N., Popa, L.D., Perișoară, L., Matei, G., Teliban, G.C. (2022). Contributions to the Mathematical Modeling of the Threshing and Separation Process in An Axial Flow Combine, *Agriculture*. 12 (10), 1520. <https://doi.org/10.3390/agriculture12101520>;
- [18] Vlăduț, N.V., Ungureanu, N., Biris, S.St., Voicea, I., Nenciu, F., Găgeanu, I., Cujbescu, D., Popa, L.D., Boruz, S., Matei, G., Ekielski, A., Teliban, G.C. (2023). Research on the identification of some optimal threshing and separation regimes in the axial flow apparatus, *Agriculture*. 13(4), 838, DOI: 10.3390/agriculture13040838, agriculture-2301663;
- [19] Wang, J., Wang, X., Li, H., He, J., Lu, C., & Liu, D. (2021). Design and experiment of rice straw chopping device for agitation sliding cutting and tearing (水稻秸秆激荡滑切与撕裂两级切割粉碎装置设计与试验). *Transactions of the Chinese Society for Agricultural Machinery*, 52(10), 28–40.
- [20] Wei, L. (2024). Analysis on the application of rice harvesting loss reduction technology (水稻机收减损技术应用分析) *South China Agricultural Machinery*, 55(08), 57-59+80
- [21] Xu, L., Li, Y., & Ding, L. (2008). Contact mechanics analysis of the collision process between rice grains and threshing elements (水稻谷粒与脱粒元件碰撞过程的接触力学分析). *Transactions of the Chinese Society of Agricultural Engineering*, (06), 146–149.

- [22] Yang, R., Wang, W., Pan, Z., Qing, Y., Zhang, J., & Qi, S. (2024). Analysis and experimental study of single plant stability of potato harvesting in breeding experiment (育种马铃薯单株收获根系稳定性分析与试验). *Transactions of the Chinese Society of Agricultural Engineering*, 40(13), 25-35.
- [23] Zeng, S., Zeng, L., Liu, W., Wei, S., Tu, Q., & Chen, H. (2022). Design and experiment of rigid-flexible coupling rod tooth threshing device of harvester for ratooning rice (再生稻收割机刚柔耦合杆齿脱粒装置的设计与试验). *Journal of South China Agricultural University*, 43(5), 61–69
- [24] Zhang, L. (2022). *Research on monitoring and diagnosis system of longitudinal axial flow rice threshing and separating device* (纵轴流水稻脱粒分离装置堵塞监控及诊断系统研究). Huazhong Agricultural University.